

Synthesis and Evaluation of Thiazolyl-1*H*-benzo[*d*]imidazole Inhibitors of *Mycobacterium tuberculosis* Inosine Monophosphate Dehydrogenase

Kenia Pissinate,^{a,#} Diana Carolina Rostirolla,^{a,b,#} Laura Miranda Pinheiro,^a
Priyanka Suryadevara,^c Perumal Yogeewari,^c Dharmarajan Sriram,^c
Luiz Augusto Basso,^{a,b} Pablo Machado^{*,a,d} and Diógenes Santiago Santos^{*,a,b}

^aCentro de Pesquisas em Biologia Molecular e Funcional (CPBMF), Instituto Nacional de Ciência e Tecnologia em Tuberculose (INCT-TB), Pontifícia Universidade Católica do Rio Grande do Sul, 90619-900 Porto Alegre-RS, Brazil

^bPrograma de Pós-Graduação em Medicina e Ciências da Saúde, Pontifícia Universidade Católica do Rio Grande do Sul, 90619-900 Porto Alegre-RS, Brazil

^cDrug Discovery Research Laboratory, Department of Pharmacy, Birla Institute of Technology & Science-Pilani, Hyderabad Campus, 500078 Hyderabad, India

^dPrograma de Pós-Graduação em Biologia Celular e Molecular, Pontifícia Universidade Católica do Rio Grande do Sul, 90619-900 Porto Alegre-RS, Brazil

Using an orthologue-based design approach, we synthesized and assayed a series of thiazolyl-1*H*-benzo[*d*]imidazole derivatives as inhibitors of *Mycobacterium tuberculosis* inosine 5'-monophosphate dehydrogenase (*Mt*IMPDPH). From these experiments, a benzo[*d*]imidazole compound was described to inhibit the enzyme in the low micromolar range ($K_{i,IMP} = 0.55 \pm 0.02 \mu\text{M}$), which places this compound among the most potent *in vitro* *Mt*IMPDPH inhibitors developed to date. In addition, steady-state kinetic measurements and docking simulations were employed to determine its inhibition and interaction modes. The results described herein may be useful for the design and development of novel alternative therapeutics for tuberculosis that target *Mt*IMPDPH, a predicted to be essential (for optimal *in vitro* bacillus growth), druggable and assayable molecular target.

Key words: drug research, tuberculosis, orthologue-based design, IMPDPH inhibitors

Introduction

“Tuberculosis (TB) remains a major global health problem”. This affirmation opens the last TB report of the World Health Organization (WHO).¹ Declared since the 1990s to be a global public health emergency, human TB has stricken an estimated 9.0 million people, which resulted in 1.5 million deaths worldwide in 2013.¹ Moreover, it has been estimated that approximately one third of the world's population is currently infected with a latent or dormant form of *Mycobacterium tuberculosis* (*Mtb*), the main causative agent of TB in humans, thus increasing the number of people at risk for developing active TB due to infection reactivation.² The emergence of multi

and extensively drug-resistant strains of *Mtb* (MDR-TB and XDR-TB, respectively),³ the variable efficacy of the current vaccine *Mycobacterium bovis* bacillus Calmette-Guérin (BCG),⁴ and the increasing prevalence of TB-HIV co-infection¹ have highlighted the need for new control measures. Although innovative drugs such as bedaquiline^{5,6} and repurposing old drug classes have been described as a promising strategy to address this problem,⁷ the current therapeutic TB treatments are suboptimal and new drugs are still needed.⁸

Within this context, the identification, characterization, and validation of new molecular targets for the proposition of new drug-like compounds has been a challenge in the search for anti-mycobacterial agents.⁹ Indeed, the rate of target innovation in the past few decade has remained low for all research drug areas, with an average of approximately 5 first-against-target drugs *per year*.¹⁰ The

*e-mail: pablo.machado@pucrs.br; diogenes@pucrs.br

#These authors contributed equally to this work

study of novel targets can conduce to new molecules with novel mechanisms of action that are active against resistant and latent forms of Mtb, both of which are crucial attrition points in TB treatment.

Supported by the essentiality of most of its biosynthetic steps for optimal *in vitro* Mtb growth¹¹ and by evidence of nucleotide synthesis maintenance in latent bacillus,¹² the gene products of the purine nucleotide biosynthesis pathway have emerged as potential targets for drug development against both active and latent TB.¹³ Among the enzymes that compose this pathway, the inosine 5'-monophosphate dehydrogenase (IMPDH, EC 1.1.1.205) catalyzes the penultimate and rate-limiting step in guanine nucleotide biosynthesis: the oxidation of inosine 5'-monophosphate (IMP) to xanthosine 5'-monophosphate (XMP) and the concomitant reduction of nicotinamide adenine dinucleotide (NAD⁺) (Scheme 1).

Encoded by the *guaB2* gene (Rv3411c),¹⁴ *Mycobacterium tuberculosis* IMPDH (*Mt*IMPDH) has been predicted to be essential for optimal *in vitro* growth of *M. tuberculosis* H37Rv.^{11,15} Additionally, prokaryotic and eukaryotic IMPDHs have distinct structural features and kinetic properties, which make the development of species-selective inhibitors feasible.¹⁶ The different inhibition patterns of *Mt*IMPDH and human IMPDH type II (*Hs*IMPDH-II)¹⁷ have supported the proposition of this target for the development of alternative drugs with selective toxicity, a basic pharmacology principle. Moreover, both proteins share sequence similarity of approximately 38%, and the amino acids residues at the *Hs*IMPDH-II nicotinamide sub site that account for sensitivity to potent drugs, such as mycophenolic acid, are not conserved in the *Mt*IMPDH.¹⁸

Recently, the potential of IMPDH inhibitors in antimicrobial chemotherapy has been exploited, highlighting the applicability of this enzyme in drug discovery campaigns.¹⁹⁻²¹ These findings have described active compounds in whole cell assays that generate lead molecules that are now candidates for further development.^{14,19}

Thiazolyl-1*H*-benzo[*d*]imidazole derivatives have been identified from high-throughput screens as

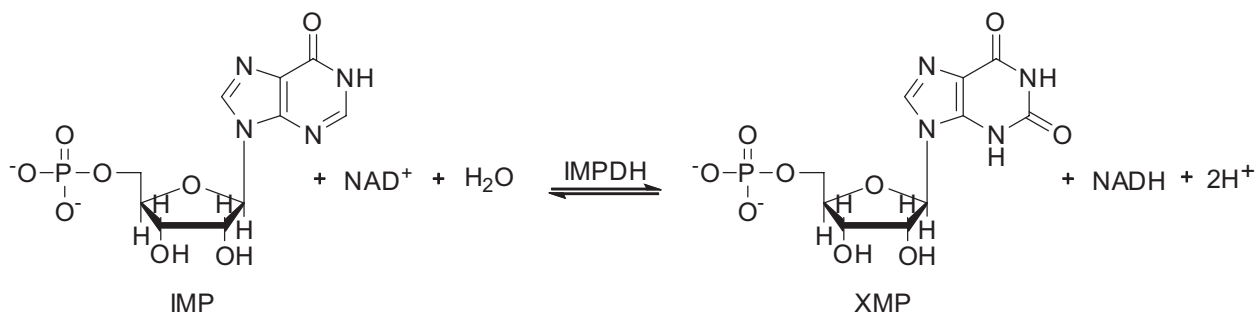
selective inhibitors of *Cryptosporidium parvum* IMPDH (*Cp*IMPDH) that target the diverged NAD⁺ site of enzyme.²² Diffraction studies from the crystal structure of *Cp*IMPDH (PDB code: 3KHJ) in complex with IMP and a benzo[*d*]imidazole-based compound (named C64) have highlighted amino acid interactions, which account for the selectivity of these compounds to *Cp*IMPDH over human IMPDH.²³ Amino acid sequence alignment of *Mt*IMPDH and *Cp*IMPDH showed that almost all of the identified residues that interact with C64 (except Ser354, which was replaced by Ala483 in *Mt*IMPDH) are conserved between the sequences (Figure S1 of the Supplementary Information). Incidentally, *Mt*IMPDH has been predicted to be sensitive to *Cp*IMPDH inhibitors¹⁶ because phylogenetic analysis points to lateral gene transfer from bacteria, thus making eukaryotic IMPDH closely related to their prokaryotic counterparts.²⁴

Therefore, there is an expected divergence between mycobacteria and host IMPDH enzymes that, taken together with the sequence conservation of binding sites, prompted us to investigate the interaction of benzo[*d*]imidazole derivatives with *Mt*IMPDH. For this, we deemed it appropriate to synthesize a series of thiazolyl-1*H*-benzo[*d*]imidazoles and evaluate their *in vitro* potential as inhibitors of *Mt*IMPDH in an orthologue-based design approach.

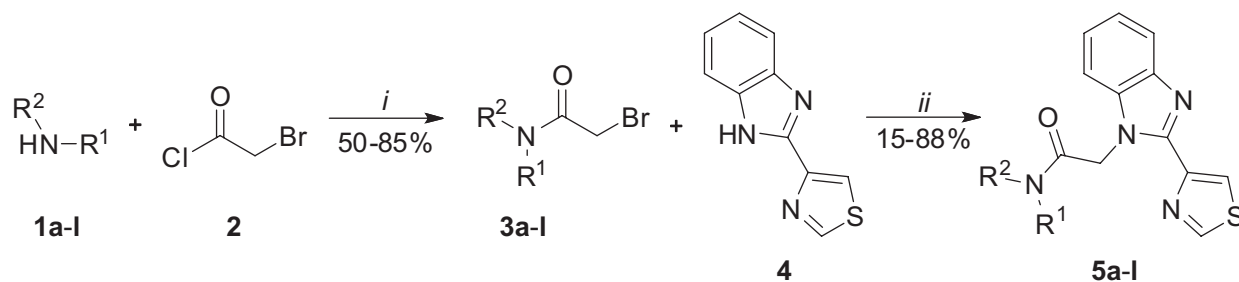
Results and Discussion

The synthesis of thiazolyl-1*H*-benzo[*d*]imidazoles was carried out in two reaction steps in accordance to previously described protocol (Scheme 2).²⁵ It is noteworthy that proposed structural modifications were aimed primarily at the creation of an electron density gradient, variation of the molecular volume, and to explore the importance of the aromaticity and planarity of the substituents in a preliminary SAR (structure activity relationship) study.

First, the classical substitution reaction of primary and secondary amines **1** at the carbonyl group of bromoacetyl chloride **2** in the presence of catalytic



Scheme 1. Chemical reaction catalyzed by IMPDH.



Compound 1,3,5	R ¹	R ²
a	Ph	H
b	4-F-C ₆ H ₄	H
c	4-Cl-C ₆ H ₄	H
d	3-Cl-C ₆ H ₄	H
e	4-Br-C ₆ H ₄	H
f	4-I-C ₆ H ₄	H
g	4-O ₂ N-C ₆ H ₄	H
h	4-NC-C ₆ H ₄	H
i	4,2-(MeO) ₂ -C ₆ H ₃	H
j	3-PrO-C ₆ H ₄	H
k	2-Me-C ₆ H ₄	H
l	CH ₂ (CH ₂) ₃ CH ₂	

Scheme 2. Reaction conditions: (i) DMAP, CH₂Cl₂, 0-25 °C, 3.5 h; (ii) K₂CO₃, DMF, 25 °C, 8 h.

amounts of 4-dimethyl aminopyridine (DMAP) conducted to 2-bromo-*N*-phenylacetamides **3a-l** with 50-85% yield. The aliphatic nucleophilic substitution (S_N2) of 2-bromo-*N*-phenylacetamides with 2-(4-thiazolyl)benzimidazole (**4**) using potassium carbonate (K₂CO₃) as base and dimethyl formamide (DMF) as solvent furnished the desired thiazolyl-1*H*-benzo[*d*]imidazoles **5a-l** with 15-88% yield. All spectroscopic and spectrometric data obtained were in agreement with the proposed structures (see Supplementary Information).

The effect of each compound on catalytic activity of recombinant *Mt*IMPDPH was evaluated by monitoring the production of NADH (nicotinamide adenine dinucleotide). First, all of the synthesized compounds were assayed at a final-fixed concentration of 10 μM, and when the inhibition was greater than 50% of the initial enzymatic activity, the IC₅₀ values (concentration of inhibitor that reduces enzyme velocity by half) were determined (Table 1).

The results shown in the Table 1 demonstrate that *Mt*IMPDPH inhibition is highly sensitive to minor modifications of the thiazolyl-1*H*-benzo[*d*]imidazoles substituent groups. Additionally, the electron withdrawing groups generally showed better inhibitory activity on recombinant *Mt*IMPDPH. Compared with the non-substituted **5a**, the replacement of hydrogen by halogens at the 4-position of the benzene ring furnished molecules with

Table 1. Inhibition of thiazolyl-1*H*-benzo[*d*]imidazoles **5a-l** on recombinant *Mt*IMPDPH activity

entry	Inhibition / % ^a	IC ₅₀ / (μmol L ⁻¹)
5a	< 2%	> 10
5b	25%	> 10
5c	67%	4.5 ± 0.4 ^b
5d	< 2%	> 10
5e	80%	3.0 ± 0.3 ^b
5f	60%	9.0 ± 3.0
5g	64%	8.0 ± 0.3
5h	50%	≥ 10
5i	< 4%	> 10
5j	65%	5.1 ± 0.5
5k	< 4%	> 10
5l	< 3%	> 10

^aObserved at a final concentration of 10 μmol L⁻¹; ^bIC₅₀ ≥ 20 μmol L⁻¹ for *Hs*IMPDPH-II.²³

improved inhibitory activity. This strategy has been extensively explored in medicinal chemistry programs aiming for more lipophilic molecules and the addition of a new site for hydrogen and/or halogen bonding. It is noteworthy that as the atomic volume of halogens increased, the inhibitory action of the compounds became

more potent (Table 1). The compound 4-fluoro substituted **5b** inhibited the enzyme activity with an $IC_{50} > 10 \mu\text{mol L}^{-1}$ (25% at $10 \mu\text{mol L}^{-1}$), whereas both 4-chloro (**5c**) and 4-bromo (**5e**) substituted compounds conducted to IC_{50} values of $4.5 \pm 0.4 \mu\text{mol L}^{-1}$ and $3.0 \pm 0.3 \mu\text{mol L}^{-1}$, respectively. Interestingly, the iodine substituted compound **5f** showed less inhibitory activity on *Mt*IMPDH than did its isostere molecules **5c** and **5e**; its IC_{50} was determined at $9.0 \pm 3.0 \mu\text{mol L}^{-1}$. The lower activity may be related to a possible steric hindrance at the 4-position of the benzene ring of thiazolyl-1*H*-benzo[*d*]imidazoles because a molecular volume-improving limit may have been achieved with the bromo-substituted **5e**. It is important to note that the replacement of the chloro group attached at the 4- to 3-position of the benzene ring led to compound **5d**, which lacked inhibition capacity on *Mt*IMPDH in our experimental conditions. This result emphasizes the fine tuning of the halogen's position relative to the *Mt*IMPDH binding site. The 4-nitro and 4-cyanobenzo[*d*]imidazole compounds (**5g**, **5h**) both showed similar inhibition activity, with an IC_{50} of $8.0 \pm 0.3 \mu\text{mol L}^{-1}$ and $\geq 10 \mu\text{mol L}^{-1}$, respectively. Focusing on the compounds substituted with electron donating groups, the results for benzo[*d*]imidazoles **5i-k** showed that only the compound carrying the 3-propoxy group (**5j**) exhibited a significant inhibition of *Mt*IMPDH activity. The IC_{50} of **5j** was $5.1 \pm 0.5 \mu\text{mol L}^{-1}$, similar to lead compound **5e**, suggesting the existence of a hydrophobic portion accessed by the mobile 3-propoxy group. Finally, the benzo[*d*]imidazole derivative from piperidine (**5l**) did not show action on catalytic *Mt*IMPDH activity in our assay conditions. Therefore, the initial screening of 12 molecules showed that five compounds (**5c**, **5e-g**, and **5j**) displayed reasonably good inhibition ($IC_{50} < 10 \mu\text{mol L}^{-1}$) on *Mt*IMPDH activity. These five

benzo[*d*]imidazoles showed no time-dependent inhibition up to 30 min of preincubation with *Mt*IMPDH suggesting rapid equilibrium processes (data not shown). It is noteworthy that compounds **5c** and **5e** showed selective *Mt*IMPDH inhibition because both have been described to show an $IC_{50} \geq 20 \mu\text{mol L}^{-1}$ for *Hs*IMPDH-II.²³

Accordingly, K_i (inhibition constant) measurements were carried out using classic Michaelis-Menten experiments. The K_i values were determined for benzo[*d*]imidazole **5e**, the lead of the series of synthesized analogs. Lineweaver-Burk plots suggested the mode of inhibition based on the effects on V_{max} (maximal velocity) and K_m (Michaelis constant) values for each inhibition type, and data fitting to appropriate equations led to values for the inhibition constants (K_{is} and/or K_{ii} ; K_{ii} is the overall inhibition constant for the enzyme-substrate-inhibitor complex, and K_{is} is the overall inhibition constant for the enzyme-inhibitor complex). Particular signatures and mechanism of inhibition for *Mt*IMPDH inhibitors were investigated and provided insights into the interaction mode for the enzyme.^{14, 17, 19}

For benzo[*d*]imidazole **5e**, the types of inhibition were characterized as uncompetitive toward IMP and noncompetitive to NAD^+ (Figure 1). Compound **5e** showed K_{is} values of $0.55 \pm 0.02 \mu\text{mol L}^{-1}$ for IMP and values of $K_{is} = 2 \pm 1 \mu\text{mol L}^{-1}$ and $K_{ii} = 0.7 \pm 0.1 \mu\text{mol L}^{-1}$ for NAD^+ . It is important to note that the inhibition profile exhibited by **5e** cannot be overcome by improving the substrate concentrations, a detrimental condition for the success of inhibitors aiming for *in vivo* activity.

A steady-state ordered BiBi kinetic mechanism has been suggested for *Mt*IMPDH, in which IMP binds first and is followed by the binding of NAD^+ and NADH dissociates first and is followed by XMP release.²⁶ After the NAD^+ binding event, a rapid electron transference forming NADH

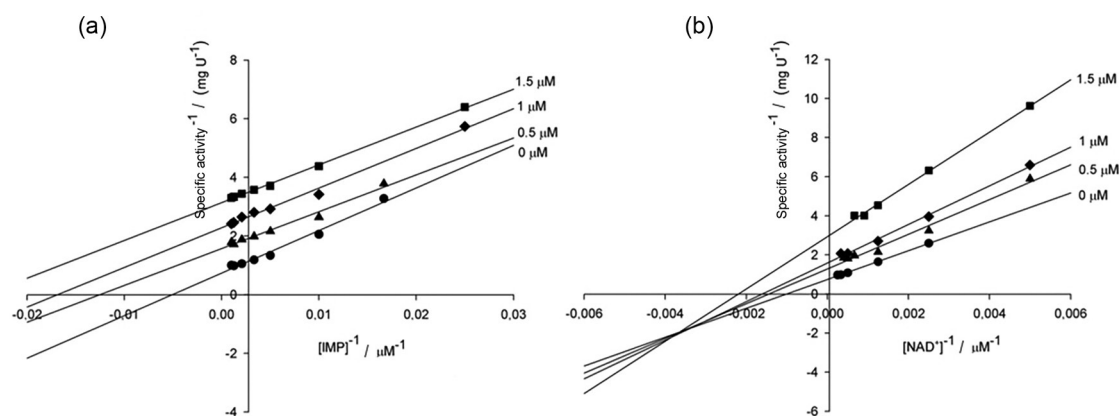


Figure 1. Double-reciprocal plots of inhibition assay for **5e**. Patterns of parallel lines indicate uncompetitive inhibition towards IMP (a), whereas intersecting lines on the left of the y-axis are indicative of noncompetitive inhibition towards NAD^+ (b). Substrate IMP was varied from 40 to 1000 $\mu\text{mol L}^{-1}$ in presence of NAD^+ 1 mmol L^{-1} (a); substrate NAD^+ was varied from 0.2 to 4 mmol L^{-1} in the presence of IMP 100 $\mu\text{mol L}^{-1}$ (b). Enzyme concentration was 550 nmol L^{-1} throughout the assays.

and the covalent intermediate E-XMP* for IMPDHs has been reported.²⁷

Similar to the analogous compounds already reported to be *Cp*IMPDH inhibitors, the inhibition pattern showed by **5e** indicates that this benzo[*d*]imidazole binds to both E-IMP and E-XMP*, with a slight preference for the E-XMP* state ($K_{is} > K_{ii}$).²² It is interesting to note that the experimental findings concerning the benzo[*d*]imidazole potencies suggest a similar interaction mode of compounds with *Mt*IMPDH to that shown by C64 with *Cp*IMPDH.²³

Finally, **5e** inhibits the *Mt*IMPDH with 50-fold less potency than *Cp*IMPDH ($IC_{50} = 0.06 \pm 0.03 \mu\text{mol L}^{-1}$).²⁵ This difference may be related to the replacement of Ser354 residue in the eukaryotic protein by Ala483 in the *Mt*IMPDH. This modification alters the physicochemical properties of the binding site because alanine is a non-polar residue replacing a polar one. Thus, the hydrogen-bonding network formed among Glu329, Ser354, Thr221 and amide group²³ would not likely occur in *Mt*IMPDH.

In order to explore the binding phenomenon, a three dimensional protein model was constructed and used for docking simulations. The necessary coordinates for the protein structure was prepared using popular method of homology modeling, details of which has been provided in the Supplementary Information. Interestingly, compound **5e** (most active out of 12) was found to be binding to the protein with best ranking and docking score of $-6.69 \text{ kcal mol}^{-1}$. The compound was found to be involved in hydrogen bonding with residues Ser83, Ser339, Ile340 and Tyr421 and also in cation- π interaction between Arg443 and phenyl ring of compound (Figure 2). Moreover, the 4-bromo phenyl group of compound was found to be stabilized by strong hydrophobic interactions with residues Met85, Cys341, Met424 and Arg443. These strong interactions of **5e** at the active site can be reasoned for its activity towards *Mt*IMPDH. While analyzing the docking pattern of inactive compounds such as **5a** and **5d** (Figure S7 of the Supplementary Information), the compounds were found to be lacking some of the polar contacts with Ile340 and Tyr421 and also Ser339. The compounds were also found to be orienting slightly in different manner, compared to **5e**, which moved the thiazole ring away from Tyr341 making it unavailable for hydrogen bonding.

Conclusions

In summary, we have reported the efficient preparation of benzo[*d*]imidazole derivatives and their use as inhibitors on catalytic activity of *Mt*IMPDH. The proposition of these compounds as possible *Mt*IMPDH inhibitors was based on their previously described action on *Cp*IMPDH conducting

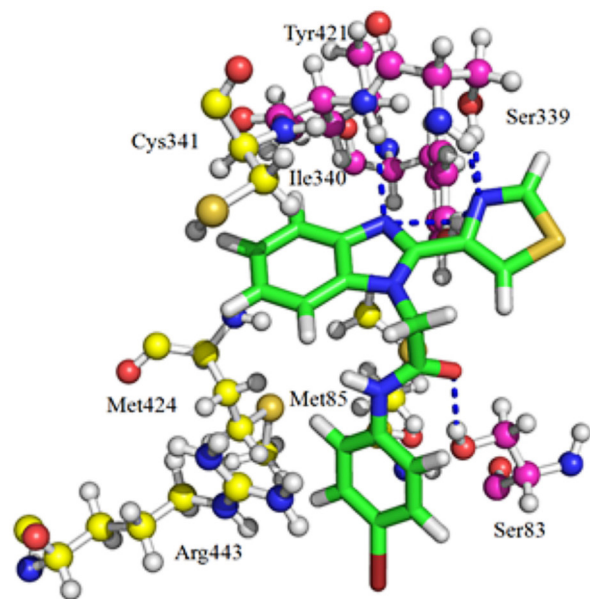


Figure 2. Interaction profile of compound **5e** (green sticks) at *Mt*IMPDH active site. Pink: residues involved in hydrogen bonding; yellow: residues involved in hydrophobic interactions; blue dashed lines indicate hydrogen bonds.

to selective inhibitors at a low micromolar range. To the best of our knowledge, the titled compounds are among the most potent *Mt*IMPDH inhibitors described to date. Therefore, the data herein presented may provide key insights into the proposition of new compounds that can be used in the further development of novel TB drugs that target *Mt*IMPDH.

Experimental

All common reactants and solvents were used as obtained from commercial suppliers without further purification. All reactions involving reactants, reagents or intermediates sensitive to air or moisture were performed under an inert atmosphere of argon. Melting points were determined using a Microquímica MQAPF-302 apparatus. ^1H NMR spectra were acquired on an Anasazi EFT-60 spectrometer (^1H at 60.13 MHz) and at 30 °C. ^{13}C NMR spectra were acquired on a Fourier 300 spectrometer of University of Caxias do Sul (UCS) in Brazil (^{13}C at 75.48 MHz) and at 25 °C. DMSO- d_6 was used as the solvent, and TMS was used as an internal standard in 5 mm samples tubes. Chemical shifts are expressed in ppm, and J values are given in Hz. High-resolution mass spectra (HRMS) were obtained for all compounds on an LTQ Orbitrap Discovery mass spectrometer from Thermo Fisher Scientific. This hybrid system combines the LTQ XL linear ion trap mass spectrometer with an Orbitrap mass analyzer. The experiments were performed using direct infusion of

the sample in a solution of acetonitrile (50%), methanol (50%), and formic acid (0.1%), with a flow of 5 $\mu\text{L min}^{-1}$ in positive-ion mode using electrospray ionization. Elemental composition calculations were performed using a specific tool included in the Qual Browser module of the Xcalibur (Thermo Fisher Scientific, release 2.0.7) software. Fourier transform infrared (FTIR) spectra were recorded using a universal attenuated total reflectance (UATR) attachment on a PerkinElmer Spectrum 100 spectrometer in the wavenumber range of 650-4000 cm^{-1} with a resolution of 4 cm^{-1} . Purity of compounds was determined by HPLC using an Äkta HPLC system of GE Healthcare® Life Sciences. HPLC analysis conditions: RP column 5 μm Nucleodur C-18 (250 \times 4.6 mm); flow rate 1.5 mL min^{-1} ; UV detection at 254 nm; 100% water (0.1% acetic acid) for 7 minutes followed by linear gradient from 100% water (0.1% acetic acid) to 90% acetonitrile/methanol (1:1, v/v) in 16 min; the last partition was maintained by 15 min and subsequently returned to 100% water (0.1% acetic acid) in 5 min remaining for additional 6 min. All evaluated compounds were > 95% pure.

General procedure for the preparation of 2-bromo-*N*-phenylacetamides **3a-l**

To a solution containing aniline **1** (0.382 g, 4.1 mmol) and a catalytic amount of dimethylaminopyridine (DMAP) (0.150 g, 30 mmol%) in dry dichloromethane (20 mL) at 0 °C was added bromoacetyl chloride **2** (0.425 mL, 5.1 mmol) dropwise. The resulting solution was stirred at 0 °C for 30 min, and the temperature was then increased to 25 °C. After stirring for an additional 3 h, the reaction mixture was diluted with diethyl ether (50 mL). All of the stirring time was accomplished under argon atmosphere. The organic layers were washed sequentially with a solution of HCl (1 mol L^{-1} , 2 \times 50 mL), water (1 \times 100 mL), saturated aqueous NaHCO_3 (3 \times 50 mL), and brine (5% m/v, 1 \times 50 mL). Finally, the organic solution was dried over anhydrous MgSO_4 and evaporated under vacuum, and the residue was purified by flash chromatography on silica gel eluting with chloroform:methanol (40:1).

General procedure for the preparation of 2-thiazol-4-yl-1*H*-benzo[*d*]imidazoles **5a-l**

Selected example for compound *N*-phenyl-2-(2-thiazol-4-yl)-1*H*-benzo[*d*]imidazole-1-yl)acetamide (**5a**).

A solution containing the 2-bromo-*N*-phenyl-acetamide **3a** (0.107 g, 0.5 mmol), of K_2CO_3 (0.540 g, 1.56 mmol), and 2-(4-thiazolyl)benzimidazole **4** (0.103 g, 0.51 mmol) in 4 mL of dimethylformamide (DMF) was stirred for 8 h at

25 °C. After, the reaction mixture was dissolved in 200 mL of distilled water. The precipitated product was filtered off, washed with water and dried under vacuum. Purification of the compound was accomplished by flash chromatography on silica gel (Macherey-Nagel, 35-70 mesh) eluting with chloroform:methanol (40:1). 2-Thiazol-4-yl-1*H*-benzo[*d*]imidazoles **5b-l** were prepared in accordance with the above described protocol.

N-Phenyl-2-(2-(thiazol-4-yl)-1*H*-benzo[*d*]imidazole-1-yl)acetamide (**5a**)

Yield 35%; mp 219-220 °C; IR (UATR) ν / cm^{-1} 1670 (C=O); $^1\text{H NMR}$ (60 MHz, $\text{DMSO-}d_6$) δ 5.72 (s, 2H, CH_2), 7.00-7.64 (m, 9H, Bi-H*, Ph-H), 8.57 (d, 1H, J 2.1, Th-H*), 9.30 (d, 1H, J 2.1 Hz, Th-H), 10.53 (br, 1H, NH); HRMS (FTMS + pESI) m/z calcd. for $\text{C}_{18}\text{H}_{14}\text{N}_4\text{OS}$ (M)⁺: 335.0961; found: 335.0946; Bi-H*: benzoimidazole hydrogens; Th-H*: thiazole hydrogens.

N-(4-Fluorophenyl)-2-(2-(thiazol-4-yl)-1*H*-benzo[*d*]imidazol-1-yl)acetamide (**5b**)

Yield 75%; mp 227- 228 °C; IR (UATR) ν / cm^{-1} 1673 (C=O); $^1\text{H NMR}$ (60 MHz, $\text{DMSO-}d_6$) δ 5.68 (s, 2H, CH_2), 6.96-7.72 (m, 8H, Bi-H*, C_6H_4), 8.57 (d, 1H, J 2.1 Hz, Th-H*), 9.30 (d, 1H, J 2.1 Hz, Th-H); HRMS (FTMS + pESI) m/z calcd. for $\text{C}_{18}\text{H}_{13}\text{FN}_4\text{OS}$ (M)⁺: 353.0867; found: 353.0847; Bi-H*: benzoimidazole hydrogens; Th-H*: thiazole hydrogens.

N-(4-Chlorophenyl)-2-(2-(thiazol-4-yl)-1*H*-benzo[*d*]imidazol-1-yl)acetamide (**5c**)

Yield 85%; mp 228-229 °C; IR (UATR) ν / cm^{-1} 1682 (C=O); $^1\text{H NMR}$ (60 MHz, $\text{DMSO-}d_6$) δ 5.71 (s, 2H, CH_2), 7.19-7.80 (m, 8H, Bi-H*, C_6H_4), 8.57 (d, 1H, J 2.1 Hz, Th-H*), 9.03 (d, 1H, J 2.1 Hz, Th-H); $^{13}\text{C NMR}$ (75 MHz, $\text{DMSO-}d_6$) δ 48.6 (CH_2), 111.1, 119.4, 121.1, 122.7, 122.8, 123.3, 127.4, 129.2, 136.9, 138.2, 142.7, 147.3, 147.5, 155.8, 166.5 (C=O); HRMS (FTMS + pESI) m/z calcd. for $\text{C}_{18}\text{H}_{13}\text{ClN}_4\text{OS}$ (M)⁺: 369.0563; found: 369.0555; Bi-H*: benzoimidazole hydrogens; Th-H*: thiazole hydrogens.

N-(3-Chlorophenyl)-2-(2-(thiazol-4-yl)-1*H*-benzo[*d*]imidazol-1-yl)acetamide (**5d**)

Yield 18%; mp 211 °C; IR (UATR) ν / cm^{-1} 1696 (C=O); $^1\text{H NMR}$ (60 MHz, $\text{DMSO-}d_6$) δ 5.72 (s, 2H, CH_2), 7.20-7.78 (m, 8H, Bi-H*, C_6H_4), 8.59 (d, 1H, J 2.1 Hz, Th-H*), 9.31 (d, 1H, J 2.1 Hz, Th-H), 10.64 (br, 1H, NH); $^{13}\text{C NMR}$ (75 MHz, $\text{DMSO-}d_6$) δ 48.0 (CH_2), 110.6, 117.4, 118.4, 118.9, 122.2, 122.3, 122.8, 123.0, 130.5, 133.1, 136.5, 140.2, 142.2, 146.8, 147.0, 155.3, 166.3 (C=O); HRMS (FTMS + pESI) m/z calcd. for $\text{C}_{18}\text{H}_{13}\text{ClN}_4\text{OS}$

(M)⁺: 369.0571; found: 369.0563; Bi-H^{*}: benzoimidazole hydrogens; Th-H^{*}: thiazole hydrogens.

N-(4-Bromophenyl)-2-(2-(thiazol-4-yl)-1*H*-benzo[*d*]imidazol-1-yl)acetamide (**5e**)

Yield 70%; mp 231 °C; IR (UATR) ν / cm⁻¹ 1682 (C=O); ¹H NMR (60 MHz, DMSO-*d*₆) δ 5.70 (s, 2H, CH₂), 7.19-7.79 (m, 8H, Bi-H^{*}, C₆H₄), 8.57 (d, 1H, *J* 2.1 Hz, Th-H^{*}), 9.30 (d, 1H, *J* 2.1 Hz, Th-H); HRMS (FTMS + pESI) *m/z* calcd. for C₁₈H₁₃BrN₄OS (M)⁺: 413.0066; found: 413.0045; Bi-H^{*}: benzoimidazole hydrogens; Th-H^{*}: thiazole hydrogens.

N-(4-Iodophenyl)-2-(2-(thiazol-4-yl)-1*H*-benzo[*d*]imidazol-1-yl)acetamide (**5f**)

Yield 43%; mp 258 °C; IR (UATR) ν / cm⁻¹ 1675 (C=O); ¹H NMR (60 MHz, DMSO-*d*₆) δ 5.89 (s, 2H, CH₂), 7.18-7.74 (m, 8H, Bi-H^{*}, C₆H₄), 8.54 (d, 1H, *J* 2.1 Hz, Th-H^{*}), 9.27 (d, 1H, *J* 2.1 Hz, Th-H); ¹³C NMR (75 MHz, DMSO-*d*₆) δ 48.0 (CH₂), 86.9, 110.7, 118.9, 121.2, 122.2, 122.3, 122.8, 136.5, 137.5, 138.6, 142.2, 146.8, 147.0, 155.3, 166.1 (C=O); HRMS (FTMS + pESI) *m/z* calcd. for C₁₈H₁₃IN₄OS (M)⁺: 460.9928; found: 460.9938; Bi-H^{*}: benzoimidazole hydrogens; Th-H^{*}: thiazole hydrogens.

N-(4-Nitrophenyl)-2-(2-(thiazol-4-yl)-1*H*-benzo[*d*]imidazol-1-yl)acetamide (**5g**)

Yield 88%; mp 167 °C; IR (UATR) ν / cm⁻¹ 1696 (C=O); ¹H NMR (60 MHz, DMSO-*d*₆) δ 5.77 (s, 2H, CH₂), 7.20-7.36 (m, 2H, Bi-H^{*}), 7.61-7.87 (m, 4H, Bi-H, C₆H₄), 8.14-8.30 (d, 2H, *J* 9.6 Hz, C₆H₄), 8.59 (d, 1H, *J* 2.1 Hz, Th-H^{*}), 9.22 (d, 1H, *J* 2.1 Hz, Th-H); ¹³C NMR (75 MHz, DMSO-*d*₆) δ 48.7 (CH₂), 110.7, 118.8, 122.1, 122.3, 122.8, 125.0, 136.4, 142.0, 142.2, 146.7, 147.0, 155.3, 167.2 (C=O); HRMS (FTMS + pESI) *m/z* calcd. for C₁₈H₁₃N₅O₃S (M)⁺: 380.0812; found: 380.0805; Bi-H^{*}: benzoimidazole hydrogens; Th-H^{*}: thiazole hydrogens.

N-(4-Cyanophenyl)-2-(2-(thiazol-4-yl)-1*H*-benzo[*d*]imidazol-1-yl)acetamide (**5h**)

Yield 66%; mp 236 °C; IR (UATR) ν / cm⁻¹ 1709 (C=O); ¹H NMR (60 MHz, DMSO-*d*₆) δ 5.70 (s, 2H, CH₂), 7.18-7.74 (m, 8H, Bi-H^{*}, C₆H₄), 8.57 (d, 1H, *J* 2.1 Hz, Th-H^{*}), 9.29 (d, 1H, *J* 2.1 Hz, Th-H); HRMS (FTMS + pESI) *m/z* calcd. for C₁₉H₁₃N₅OS (M)⁺: 360.0914; found: 360.0895; Bi-H^{*}: benzoimidazole hydrogens; Th-H^{*}: thiazole hydrogens.

N-(2,4-Dimethoxyphenyl)-2-(2-(thiazol-4-yl)-1*H*-benzo[*d*]imidazol-1-yl)acetamide (**5i**)

Yield 27%; mp 234 °C; IR (UATR) ν / cm⁻¹ 1671 (C=O); ¹H NMR (60 MHz, DMSO-*d*₆) δ 3.74 (s, 3H, OCH₃), 3.86

(s, 3H, OCH₃), 5.72 (s, 2H, CH₂), 6.35-6.62 (m, 2H, C₆H₃), 7.21-7.76 (m, 5H, Bi-H^{*}, C₆H₃), 8.57 (d, 1H, *J* 2.1 Hz, Th-H^{*}), 9.35 (d, 1H, *J* 2.1 Hz, Th-H); ¹³C NMR (75 MHz, DMSO-*d*₆) δ 48.1 (CH₂), 55.3, 55.8, 98.8, 103.9, 110.6, 118.9, 120.1, 122.3, 122.4, 122.7, 122.8, 136.3, 142.3, 146.9, 147.0, 151.0, 155.3, 156.7, 165.6 (C=O); HRMS (FTMS + pESI) *m/z* calcd. for C₂₀H₁₈N₄O₃S (M)⁺: 395.1172; found: 395.1177; Bi-H^{*}: benzoimidazole hydrogens; Th-H^{*}: thiazole hydrogens.

N-(3-Propoxyphenyl)-2-(2-(thiazol-4-yl)-1*H*-benzo[*d*]imidazol-1-yl)acetamide (**5j**)

Yield 15%; mp 223 °C; IR (UATR) ν / cm⁻¹ 1686 (C=O); ¹H NMR (60 MHz, DMSO-*d*₆) δ 0.93 (t, 3H, *J* 7 Hz, CH₃), 1.65 (quint, 2H, *J* 7 Hz, CH₂), 3.84 (t, 2H, *J* 7 Hz, CH₂), 5.75 (s, 2H, CH₂), 6.53-7.67 (m, 8H, Bi-H^{*}, C₆H₄), 8.56 (d, 1H, *J* 2.1 Hz, Th-H^{*}), 9.30 (d, 1H, *J* 2.1 Hz, Th-H); 10.42 (br, 1H, NH); ¹³C NMR (75 MHz, DMSO-*d*₆) δ 10.4, 22.0, 48.0 (CH₂), 68.8, 105.2, 109.5, 111.1, 122.3, 122.8, 129.6, 140.0, 159.0, 165.9 (C=O); HRMS (FTMS + pESI) *m/z* calcd. for C₂₁H₂₀N₄O₂S (M)⁺: 393.1380; found: 393.1378; Bi-H^{*}: benzoimidazole hydrogens; Th-H^{*}: thiazole hydrogens.

2-(2-(Thiazol-4-yl)-1*H*-benzo[*d*]imidazol-1-yl)-*N*-o-tolylacetamide (**5k**)

Yield 40%; mp 165 °C; IR (UATR) ν / cm⁻¹ 1666 (C=O); ¹H NMR (60 MHz, DMSO-*d*₆) δ 2.21 (s, 3H, CH₃), 5.70 (s, 2H, CH₂), 6.91-7.77 (m, 8H, Bi-H^{*}, C₆H₄), 8.53 (d, 1H, *J* 2.1 Hz, Th-H^{*}), 9.30 (d, 1H, *J* 2.1 Hz, Th-H), 9.71 (br, 1H, NH); HRMS (FTMS + pESI) *m/z* calcd. for C₁₉H₁₆N₄OS (M)⁺: 349.1118; found: 349.1122; Bi-H^{*}: benzoimidazole hydrogens; Th-H^{*}: thiazole hydrogens.

1-(Piperidin-1-yl)-2-(2-(thiazol-4-yl)-1*H*-benzo[*d*]imidazol-1-yl)ethanone (**5l**)

Yield 44%; mp 171 °C; IR (UATR) ν / cm⁻¹ 1642 (C=O); ¹H NMR (60 MHz, DMSO-*d*₆) δ 1.63 (br, 6H, Pi-H^{*}), 3.51 (br, 6H, Pi-H), 5.64 (s, 2H, CH₂), 7.25-7.81 (m, 4H, Bi-H^{*}), 8.31 (d, 1H, *J* 2.1 Hz, Th-H^{*}), 8.83 (d, 1H, *J* 2.1 Hz, Th-H); ¹³C NMR (75 MHz, DMSO-*d*₆) δ 24.1, 25.3, 25.9, 42.7, 45.4, 46.4, 110.6, 118.7, 122.0, 122.2, 122.6, 136.5, 142.0, 146.9, 147.1, 155.0, 164.9 (C=O); HRMS (FTMS + pESI) *m/z* calcd. for C₁₇H₁₈N₄OS (M)⁺: 327.1274; found: 327.1273; Pi-H: piperidine hydrogens; Bi-H^{*}: benzoimidazole hydrogens; Th-H^{*}: thiazole hydrogens.

Enzymatic activity assays

The recombinant *Mt*IMPDPH was expressed and purified as previously described.²⁶ The effect of each compound on steady-state velocities was evaluated using

a UV-2550 UV-Visible spectrophotometer (Shimadzu) by monitoring NAD⁺ reduction to NADH at 340 nm ($\epsilon_{\beta\text{-NADH}}$: 6.22 M⁻¹ cm⁻¹) and corrected for non-catalyzed chemical reactions in the absence of *Mt*IMPDH. Assays were performed at 37 °C, in 50 mmol L⁻¹ Tris pH 8.5, 1 mmol L⁻¹ DTT, and 200 mmol L⁻¹ KCl. Enzyme-catalyzed reaction started with the addition of *Mt*IMPDH at 145 nM to the assay mixture (500 μL of final volume) and data were collected for 5 min. The inhibitors were dissolved in dimethyl sulfoxide (DMSO) and added to the reaction mixture at a final concentration of 10 μmol L⁻¹. Enzyme velocity was used to determine the % inhibition and, as a control, the maximal rate of the enzymatic reaction (100% of *Mt*IMPDH activity) was determined in the absence of inhibitor and in the presence of fixed non-saturating concentrations of IMP (100 μmol L⁻¹, $K_{0.5}$ ca. 120 μmol L⁻¹) and NAD⁺ (1 mmol L⁻¹, K_m ca. 887 μmol L⁻¹), in the presence of 1% DMSO.²⁶ Compounds able to reduce the enzyme activity by more than 50% were selected for further IC₅₀ determination.

IC₅₀ determinations

The IC₅₀ values were determined by adding different concentrations of the compounds (dissolved in DMSO) to the reaction mixture above described and the enzyme velocity was used to determine the % inhibition. The IC₅₀ values were estimated using equation 1, where [I] is the inhibitor concentration, v_i is the initial velocity in the presence of the inhibitor, v_0 is the initial velocity in the absence of inhibitor, and the IC₅₀ value is defined as the concentration of the inhibitor that reduces the enzyme velocity by half.

$$\frac{v_i}{v_0} = \frac{1}{1 + \left(\frac{[I]}{IC_{50}} \right)} \quad (1)$$

Time-dependent inhibition

To evaluate whether or not enzyme inhibition may be time dependent, recombinant *Mt*IMPDH was preincubated at room temperature with 10 μmol L⁻¹ inhibitor (final concentration), which was then added at different times (up to 30 min) to the reaction mixture, as previously described. This analysis was performed to determine if inhibition follows a rapid equilibrium mode (classical competitive, uncompetitive and noncompetitive inhibition) or if there is a slow step in the equilibrium process.

Mode of inhibition and determination of the overall inhibition constant for **5e**

The determination of K_i values and the mode of inhibition were performed for **5e** inhibitor towards both *Mt*IMPDH substrates. Lineweaver-Burk (double-reciprocal) plots were employed to determine the mode of inhibition (competitive, noncompetitive or uncompetitive) and data fitting to appropriate equations gave values for the inhibition constants (K_{is} and/or K_{ii}). In short, the inhibition mode was proposed based on the effects on V_{max} and K_m values for each inhibition type, resulting in plots with distinct straight line patterns toward either IMP or NAD⁺ as follows: lines intercept on y axis for competitive inhibition (does not affect the apparent V_{max} and increases apparent K_m), lines intercept on left of y axis for noncompetitive inhibition (decreases apparent V_{max} , and does not affect apparent K_m values if $K_{is} = K_{ii}$, increases the apparent K_m values if $K_{is} < K_{ii}$, or decreases the K_m values if $K_{is} > K_{ii}$), and parallel lines for uncompetitive inhibition (decreases both apparent V_{max} and K_m values).²⁸

The inhibition studies were carried out at varying concentrations of one substrate, a fixed non-saturating concentration of the other substrate, and in the absence of inhibitor and in the presence of three different concentrations of each inhibitor **5e** (0.5, 1 and 1.5 μmol L⁻¹). For IMP substrate analysis, the experiment was carried out with IMP concentrations ranging from 40 μmol L⁻¹ to 1000 μmol L⁻¹ and NAD⁺ at 1 mmol L⁻¹; for NAD⁺ substrate analysis, the NAD⁺ concentrations ranged from 0.2 mmol L⁻¹ to 4 mmol L⁻¹, with IMP fixed at 100 μmol L⁻¹. The enzyme concentration was constant at 550 nM throughout the assays. Noncompetitive and uncompetitive inhibition data were fitted to equations 2 and 3, respectively:

$$\frac{1}{v_0} = \frac{K_m}{V_{max}} \left(1 + \frac{I}{K_{is}} \right) \left(\frac{1}{[S]} \right) + \frac{1}{V_{max}} \left(1 + \frac{[I]}{K_{ii}} \right) \quad (2)$$

$$\frac{1}{v_0} = \frac{K_m}{V_{max}} \left(\frac{1}{[S]} \right) + \frac{1}{V_{max}} \left(1 + \frac{[I]}{K_{ii}} \right) \quad (3)$$

In these equations, [I] is the inhibitor concentration, [S] is the substrate concentration, K_m is the Michaelis constant, V_{max} is the maximal velocity, and K_{ii} is the overall inhibition constant for the enzyme-substrate-inhibitor complex, and K_{is} is the overall inhibition constant for the enzyme-inhibitor complex.²⁸

Computational studies

Homology modeling is used to predict the three-dimensional structure of a protein sequence.

Until date there were no crystal structure reported for *Mt*IMPDPH, which motivate us for protein modeling using one of its close homolog crystal structure with maximum identity as template. The *Mt*IMPDPH protein sequence was retrieved from Swiss-Prot protein database (accession id: P9WKI7.1).²⁹ A similarity search was done for the protein sequence against protein data bank using BLAST (Basic Local Alignment Search Tool).³⁰ This search resulted in identification of crystal structure of IMPDPH with XMP from *Bacillus anthracis str. Ames* (PDB ID-3TSD) with 54% identity to *Mt*IMPDPH sequence.³¹ This was the template identified with maximum identity. The homology model for *Mt*IMPDPH was generated using Prime v2.3 of Schrödinger 2012.³² Crystal ligand coordinates from template were also incorporated into model during model development. The model generated was subjected to loop refinement and finally the energy was minimized using the OPLS-2005 force field.³³ The developed model was inspected for Ramachandran plot using PROCHECK analysis.³⁴ The ProSA analysis was done for the final model so as to study the overall quality of the model.³⁵ The root mean square deviation (rmsd) of model when superimposed over the template was also checked so as to assess the reliability of model. Further, the active site of the model was analyzed based on the sequence alignment and SiteMap v2.6 of Schrödinger 2012.³⁶ More information regarding the homology modeling can be obtained in Supplementary Information.

Molecular docking studies for the synthesized 12 compounds were carried out with the modeled protein using Glide v5.8 of Schrödinger 2012.³⁷ The compounds for docking were sketched using Maestro panel of Schrodinger and their geometry was cleaned and all possible confirmations were generated using LigPrep v2.5 of Schrödinger.³⁷ Finally, the resulted docking poses for the compounds with the protein were analyzed for active site interactions.

Supplementary Information

Supplementary Information (amino acid sequence alignment of *Mt*IMPDPH and *Cp*IMPDPH, ¹H NMR spectra of compounds, ¹³C NMR spectra of selected compounds, and more details of the computational studies) is available free of charge at <http://jbc.sbj.org.br> as PDF file.

Acknowledgements

This work was supported by funds from the National Institute of Science and Technology on Tuberculosis (INCT-TB), Decit/SCTIE/MS-MCT-CNPq-FNDCT-

CAPES (Brazil) to D. S. Santos and L. A. Basso. L. A. Basso and D. S. Santos are Research Career Awardees of the National Research Council of Brazil (CNPq). The fellowships from CNPq (D. C. Rostirolla, K. Pissinate, and L. M. Pinheiro), and from special visiting researcher program are also acknowledged. Finally, P. Yogeewari acknowledges Department of Biotechnology for their financial assistance.

References

1. World Health Organization (WHO); *Global Tuberculosis Report 2014*; WHO Press: Geneva, 2014. Available in: http://www.who.int/tb/publications/global_report/en/ accessed in April 2015.
2. Barry, C. E.; Boshoff, H. I.; Dartois, V.; Dick, T.; Ehrh, S.; Flynn, J.; Schnappinger, D.; Wilkinson, R. J.; Young, D.; *Nat. Rev. Microbiol.* **2009**, *7*, 845.
3. Gandhi, N. R.; Nunn, P.; Dheda, K.; Schaaf, H. S.; Zignol, M.; Soolingen, D. V.; Jensen, P.; Bayona, J.; *Lancet* **2010**, *375*, 1830.
4. Colditz, G. A.; Brewer, T. F.; Berkey, C. S.; Wilson, M. E.; Burdick, E.; Fineberg, H. V.; Mosteller, F.; *J. Am. Med. Assoc.* **1994**, *271*, 698.
5. Diacon, A. H.; Pym, A.; Grobusch, M.; Patientia, R.; Rustomjee, R.; Page-Shipp, L.; Pistorius, C.; Krause, R.; Bogoshi, M.; Churchyard, G.; Venter, A.; Allen, J.; Palomino, J. C.; De Marez, T.; van Heeswijk, R. P. G.; Lounis, N.; Meyvisch, P.; Verbeeck, J.; Parys, W.; Beule, K.; Andries, K.; Mc Neeley, D. F. N.; *N. Engl. J. Med.* **2009**, *360*, 2397.
6. Avorn, J.; *J. Am. Med. Assoc.* **2013**, *309*, 1349.
7. Zumla, A.; Nahid, P.; Cole, S. T.; *Nat. Rev. Drug Discovery* **2013**, *12*, 388.
8. Koul, A.; Arnoult, E.; Lounis, N.; Guillemont, J.; Andries, K.; *Nature* **2011**, *469*, 483.
9. Hasan, S.; Daugelat, S.; Rao, P. S. S.; Schreiber, M.; *PLoS Comput. Biol.* **2006**, *2*, e61.
10. Overington, J. P.; Al-Lazikani, B.; Hopkins, A. L.; *Nat. Rev. Drug Discovery* **2006**, *5*, 993.
11. Sasseti, C. M.; Boyd, D. H.; Rubin, E. J.; *Mol. Microbiol.* **2003**, *48*, 77.
12. Boshoff, H. I. M.; Barry, C. E.; *Nat. Rev. Microbiol.* **2005**, *3*, 70.
13. Ducati, R. G.; Breda, A.; Basso, L. A.; Santos, D. S.; *Curr. Med. Chem.* **2011**, *18*, 1258.
14. Usha, V.; Gurucha, S. S.; Lovering, A. L.; Lloyd, A. J.; Papaemmanouil, A.; Reynolds, R. C.; Besra, G. S.; *Microbiology* **2011**, *157*, 290.
15. Jesus, M. A.; Zhang, Y. J.; Sasseti, C. M.; Rubin, E. J.; Sacchettini, J. C.; Loerger, T. R.; *Bioinformatics* **2013**, *29*, 695.
16. Hedstrom, L.; Liechti, G.; Goldberg, J. B.; Gollapalli, D. R.; *Curr. Med. Chem.* **2011**, *18*, 1909.

17. Chen, L.; Wilson, D. J.; Xu, Y.; Aldrich, C. C.; Felczak, K.; Sham, Y. Y.; Pankiewicz, K. W.; *J. Med. Chem.* **2010**, *53*, 4768.
18. Sintchak, M. D.; Fleming, M. A.; Futer, O.; Raybuck, S. A.; Chambers, S. P.; Caron, P. R.; Murcko, M. A.; Wilson, K. P.; *Cell* **1996**, *85*, 921.
19. Usha, V.; Hobrath, J. V.; Gurucha, S. S.; Reynolds, R. C.; Besra, G. S.; *PLoS One* **2012**, *7*, e33886.
20. Johnson, C. R.; Gorla, S. K.; Kavitha, M.; Zhang, M.; Liu, X.; Striepen, B.; Mead, J. R.; Cuny, G. D.; Hedstrom, L.; *Bioorg. Med. Chem. Lett.* **2013**, *23*, 1004.
21. Gorla, S. K.; Kavitha, M.; Zhang, M.; Chin, J. E. W.; Liu, X.; Striepen, B.; Makowska-Grzyska, M.; Kim, Y.; Joachimiak, A.; Hedstrom, L.; Cuny, G. D.; *J. Med. Chem.* **2013**, *56*, 4028.
22. Umejiego, N. N.; Gollapalli, D.; Sharling, L.; Volftsun, A.; Lu, J.; Benjamin, N. N.; Stroupe, A. H.; Riera, T. V.; Striepen, B.; Hedstrom, L.; *Chem. Biol.* **2008**, *15*, 70.
23. MacPherson, I. S.; Kirubakaran, S.; Gorla, S. K.; Riera, T. V.; D'Aquino, J. A.; Zhang, M.; Cuny, G. D.; Hedstrom, L.; *J. Am. Chem. Soc.* **2010**, *132*, 1230.
24. Striepen, B.; White, M. W.; Li, C.; Guerini, M. N.; Malik, S. B.; Logsdon, J. M. J.; Liu, C.; Abrahamsen, M. S.; *Proc. Natl. Acad. Sci. U.S.A* **2002**, *99*, 6304.
25. Kirubakaran, S.; Gorla, S. K.; Sharling, L.; Zhang, M.; Liu, X.; Ray, S. S.; MacPherson, I. S.; Striepen, B.; Hedstrom, L.; Cuny, G. D.; *Bioorg. Med. Chem. Lett.* **2012**, *22*, 1985.
26. Rostirolla, D. C.; Assunção, T. M.; Bizarro, C. V.; Basso, L. A.; Santos, D. S.; *RSC Adv.* **2014**, *4*, 26271.
27. Hedstrom, L.; *Chem. Rev.* **2009**, *109*, 2903.
28. Cleland, W. W.; Cook, P. F.; *Enzyme Kinetics and Mechanism*; Garland Science Publishing: New York, 2007.
29. Cole, S.; Brosch, R.; Parkhill, J.; Garnier, T.; Churcher, C.; Harris, D.; Gordon, S. V.; Eiglmeier, K.; Gas, S.; Barry, C. E.; Tekaia, F.; Badcock, K.; Basham, D.; Brown, D.; Chillingworth, T.; Connor, R.; Davies, R.; Devlin, K.; Feltwell, T.; Gentles, S.; Hamlin, N.; Holroyd, S.; Hornsby, T.; Jagels, K.; Krogh, A.; McLean, J.; Moule, S.; Murphy, L.; Oliver, K.; Osborne, J.; Quail, M. A.; Rajandream, M. A.; Rogers, J.; Rutter, S.; Seeger, K.; Skelton, J.; Squares, R.; Squares, S.; Sulston, J. E.; Taylor, K.; Whitehead, S.; Barrell, B. G.; *Nature* **1998**, *393*, 537.
30. Altschul, S. F.; Gish, W.; Miller, W.; Myers, E. W.; Lipman, D. J.; *J. Mol. Biol.* **1990**, *215*, 403.
31. Makowska-Grzyska, M.; Kim, Y.; Wu, R.; Wilton, R.; Gollapalli, D. R.; Wang, X. K.; Zhang, R.; Jedrzejczak, R.; Mack, J. C.; Maltseva, N.; Mulligan, R.; Binkowski, T. A.; Gornicki, P.; Kuhn, M. L.; Anderson, W. F.; Hedstrom, L.; Joachimiak, A.; *Biochemistry* **2012**, *51*, 6148.
32. *Prime version 2.3*, Schrödinger; LLC, New York, 2012.
33. Banks, J. L.; Beard, H. S.; Cao, Y.; Cho, A. E.; Damm, W.; Farid, R.; Felts, A. K.; Halgren, T. A.; Mainz, D. T.; Maple, J. R.; Murphy, R.; Philipp, D. M.; Repasky, M. P.; Zhang, L. Y.; Berne, B. J.; Friesner, R. A.; Gallicchio, E.; Levy, R. M.; *J. Comput. Chem.* **2005**, *26*, 1752.
34. Laskowski, R. A.; McArthur, M. W.; Moss, D. S.; Thornton, J. M.; *J. Appl. Cryst.* **1993**, *26*, 283.
35. Wiederstein, M.; Sippl, M. J.; *Nucleic Acids Res.* **2007**, *35*, W407.
36. *SiteMap version 2.6*, Schrödinger; LLC, New York, 2012.
37. *Glide, version 5.8*, Schrödinger; LLC, New York, 2012; *LigPrep, version 2.5*, Schrödinger; LLC, New York, 2012.

Submitted: January 16, 2015

Published online: April 30, 2015

FAPERGS has sponsored the publication of this article.